Step bunching instability and its effects in electrocatalysis on platinum surfaces

Valls Mascaró, F; Koper, M.T.M.; Rost, M.J.

nature catalysis

Article

https://doi.org/10.1038/s41929-024-01232-2

Step bunching instability and its effects in electrocatalysis on platinum surfaces

Received: 15 March 2024

Accepted: 4 September 2024

Published online: 30 September 2024

Check for updates

Francesc Valls Mascaró [1], Marc T. M. Koper[1] & Marcel J. Rost [2]

The atomic-scale surface structure plays a major role in the electrochemical behaviour of a catalyst. The electrocatalytic activity towards many relevant reactions, such as the oxygen reduction reaction on platinum, exhibits a linear dependency with the number of steps until this linear scaling breaks down at high step densities. Here we show, using Pt(111)-vicinal surfaces and in situ electrochemical scanning tunnelling microscopy, that this anomalous behaviour at high step densities has a structural origin and is attributed to the bunching of closely spaced steps. While Pt(554) presents parallel single steps and terrace widths that correspond to its nominal, expected value, most steps on Pt(553) are bunched. Our findings challenge the common assumption in electrochemistry that all stepped surfaces are composed of homogeneously spaced steps of monoatomic height and can successfully explain the anomalous trends documented in the literature linking step density to both activity and potential of zero total charge.

Stepped platinum single crystals are widely used in electrochemistry to study the unique reactivity of step sites. Low-energy electron diffraction, He-beam diffraction and scanning tunnelling microscopy studies in ultrahigh vacuum confirmed that Pt(111)-vicinal surfaces such as Pt(997) prepared by sputtering and annealing are stable at moderate temperatures, as long as oxygen is not present while the sample is hot[1–4]. Unfortunately, there is scarce work on the atomic-scale characterization of stepped surfaces when prepared by flame annealing (in air) and cooled down in a reducing atmosphere, which is the typical methodology followed in electrochemistry[5]. Herrero and co-workers showed that Pt(10 10 9) and Pt(11 10 10) (both with steps along a direction equivalent to [110], but with the former having {111} and the latter having {100} microfacets) present their nominal structures if an Ar + H_2 mixture is used while cooling down the samples[6]. As a result, it is often assumed in single-crystal electrochemistry studies that all stepped surfaces are composed of parallel-running monoatomic-height steps.

This assumption, however, is inconsistent with many experimental observations that show a dissimilar relation to the density of step (or step-related) sites among different Pt(111)-vicinal surfaces. For example, the potential at which the total charge is zero (E_{pztc}) decreases linearly with the step density, as expected, but only until a certain critical value, from which on it deviates substantially[7]. Similarly, the linear scaling between the oxygen reduction reaction (ORR) activity and the step density breaks down for stepped surfaces with very small terraces[8,9]. This phenomenon suggests a structural difference of the steps depending on the terrace width, despite the lack of supporting evidence in the literature.

In this Article, we offer an explanation for this anomalous behaviour. Using our electrochemical scanning tunnelling microscope (EC-STM), we show that Pt(554) exhibits exclusively single, monoatomic-height steps, while a stepped surface with theoretically narrow terraces, like Pt(553), shows mainly double-height (bunched) steps and terraces with twice the nominal width. Based on this observation, we quantitatively show, on the example of the E_{pztc} and the ORR activity, that step bunching can successfully explain the anomalous behaviour of surfaces with high step density.

Results

Thermodynamics of stepped surfaces

At thermodynamic equilibrium, the surface morphology always conforms to the one with the lowest free energy. For a surface with a high Miller index, the surface free energy at a temperature T is given by[10]

$$f_{\mathrm{total}}(T) = f_{\mathrm{terr}}(T) + f_{\mathrm{step}}(T)\frac{1}{L} + B_{\mathrm{step}}(T)\frac{1}{aL^3}, \quad (1)$$

[1]Leiden Institute of Chemistry, Leiden University, Leiden, The Netherlands. [2]Huygens-Kamerlingh Onnes Laboratory, Leiden University, Leiden, The Netherlands. e-mail: Rost@Physics.LeidenUniv.nl

https://doi.org/10.1038/s41929-024-01232-2

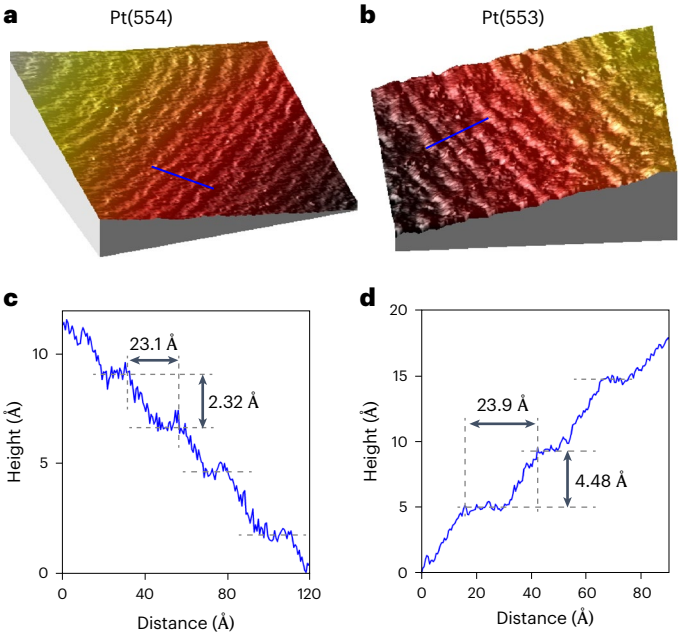

Fig. 1 | EC-STM measurements of Pt(111)-vicinal surfaces. a,**b**, 3D-rendered EC-STM images of Pt(554) (**a**) and Pt(553) (**b**), recorded in 0.1 M $HClO_4$ with $U_s = 0.1$ V and $U_t = 0.15$ V. Both images are 48 × 48 nm^2. The blue lines crossing the steps on Pt(554) and Pt(553) indicate the positions of the corresponding height lines shown in **c** and **d**. **c**,**d**, Height lines traced perpendicular to the steps on Pt(554) (**c**) and Pt(553) (**d**). Note that the step height on Pt(553) is twice the value of the steps on Pt(554) as well as that both surfaces do show an almost equal terrace width, although it should be theoretically 46% smaller on Pt(553).

where f_{terr} corresponds to the free energy of the terraces and f_{step} is the free energy of the steps, which is divided by the terrace width (L) to account for the step density. The third term describes the interactions between steps, where B_{step} is an interaction coefficient and a the unit step length ($a = 2.78$ Å).

The temperature dependance is especially important for f_{step}, as all steps at any $T > 0$ K are rough: thermally activated kinks form enabling the steps to meander, thereby increasing their entropy and lowering their free energy f_{step} according to[11]

$$f_{step}(T) = f^0_{step} - \frac{2kT}{a}\exp\left(\frac{-f^0_{kink}}{kT}\right), \quad (2)$$

where f^0_{step} and f^0_{kink} are the formation energies of a unit step length and a kink site, respectively, while k is the Boltzmann's constant. Note that at a high enough T the exponential term in equation (2) becomes practically equal to 1, which can lead to $f_{step} < 0$, that is, the surface can form steps spontaneously, describing the three-dimensional (3D) roughening transition[12].

Step meandering is, however, hindered by the step–step interaction, which has three different components. The first one is an entropic repulsion originating from the geometric confinement of a step in between its two neighbours[13,14]. The second one is an electrostatic interaction between electric dipoles that form at step edges owing to the Smoluchowski effect[15,16], which goes hand in hand with an elastic interaction[17–20]. Unlike the entropic repulsion, the electrostatic and elastic interactions are always repulsive for neighbouring steps of the same type (ascending or descending), while they can be either repulsive or attractive for the opposite type of step, depending on the strength of the dipole moment parallel to the surface[11]. In any case, all three contributions of the step–step interaction usually decay with L^{-2} (refs. 16,21). Scaling this factor to units of energy/area, we obtain the L^{-3} dependency reflected in the third term of equation (1).

Surface characterization

Figure 1a,b shows 3D-rendered EC-STM images of a Pt(554) surface and a Pt(553) surface recorded at constant sample and tip potentials, $U_s = 0.1$ V and $U_t = 0.15$ V, respectively, which we processed on the terrace planes to bring out the natural tilt of each sample (Supplementary Note 1 and Supplementary Fig. 1).

When comparing both images, one notices that the average separation between the steps, the brighter parallel lines, is similar on both surfaces, which is supported by the corresponding height lines shown in Fig. 1c,d: the terraces selected on Pt(554) and Pt(553) measure 23.1 Å and 23.9 Å in width, respectively. This is surprising, as Pt(553) naturally has double the step density of Pt(554). In fact, the theoretical terrace widths are 22.4 Å and 10.4 Å, respectively, as given by the ball model equation

$$L = \frac{\sqrt{3}}{2}d(n-1) + \frac{\sqrt{3}}{3}d, \quad (3)$$

where d is the distance between two closely packed platinum atoms and n is the number of atom rows in a single terrace ($n = 10$ for Pt(554) and $n = 5$ for Pt(553)). As the steps cannot simply vanish, because the natural surface orientation must always be preserved, the only possible explanation for the doubling of the terrace width on Pt(553) is that the steps bunch together in pairs, as illustrated in Fig. 2. Evidence for this is the step height of 4.48 Å measured in Fig. 1d, which is twice the theoretical (111) step height of 2.27 Å.

To quantify our observation statistically, we traced over 50 randomly chosen height lines from which we measured the step heights and terrace widths for both Pt(554) and Pt(553), analysing several STM images that were recorded in different experiments (Supplementary Figs. 2–5). Figure 3a shows the resulting terrace width distribution for Pt(554). Its Gaussian shape indicates the existence of a repulsive interaction between the closely spaced steps, as opposed to an asymmetric peak that would be characteristic for freely fluctuating steps[10,13]. The width of the distribution, often defined as its standard deviation (σ), depends on the interplay between f_{step} and B_{step}: a lower B_{step}, lower f^0_{kink} or a higher T results in a broader peak, as it costs less energy for the steps to wander further away from the midway position between their neighbours. From the Gaussian fit in red, we obtain $\sigma = 4.2$ Å, which is higher than the $\sigma = 2.9$ Å reported for Pt(997) in vacuum[4]. This is what we would expect, not only because the terraces on Pt(554) are one atom row wider than on Pt(997), but also because of the screening of the dipole by the electrolyte, both resulting in a lower step–step repulsive

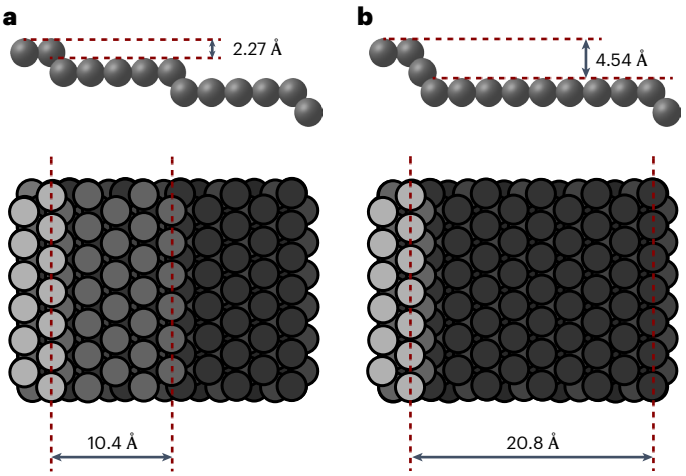

Fig. 2 | Ball model of a Pt(553) surface. a, The model with single steps. **b**, The model with double (bunched) steps. The step heights and terrace widths are indicated.

https://doi.org/10.1038/s41929-024-01232-2

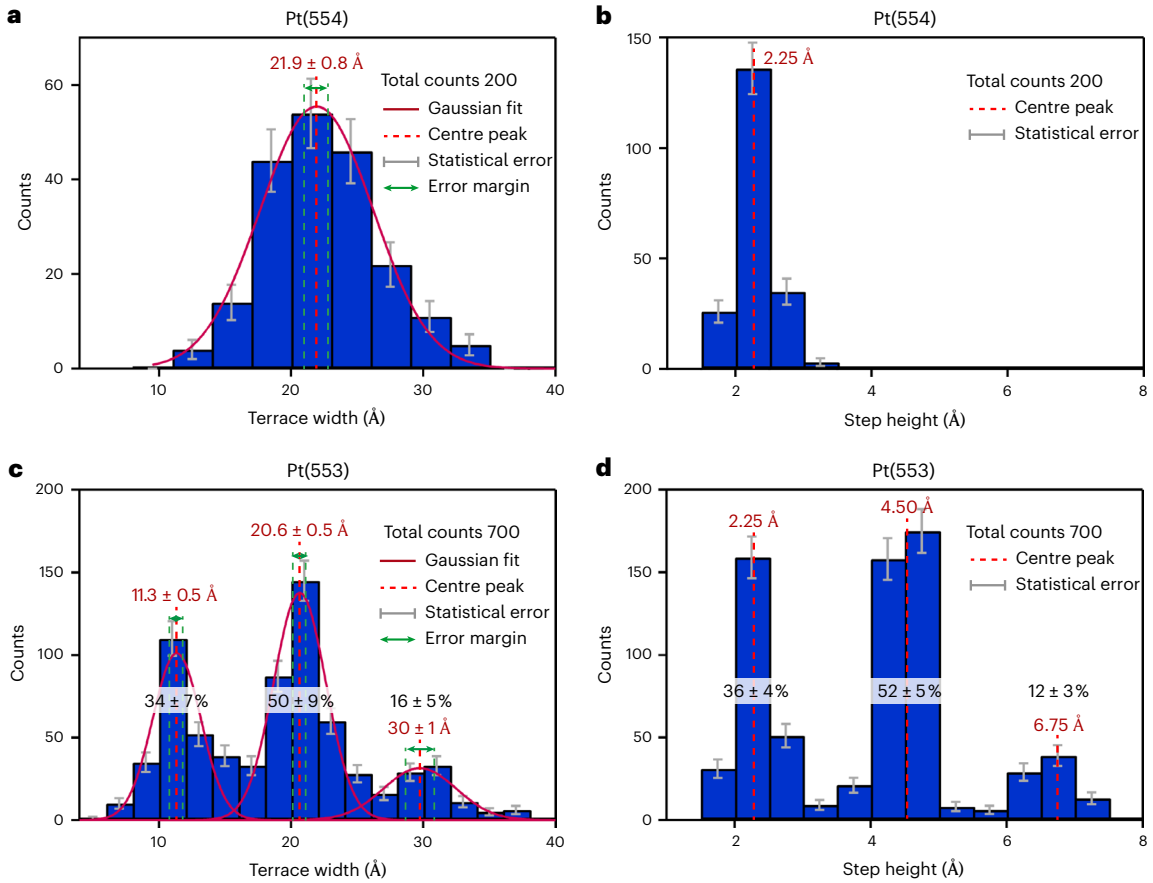

Fig. 3 | Statistical analysis of the surface structure. a,**b**, The terrace width (**a**) and step height (**b**) distributions of Pt(554). **c**,**d**, The terrace width (**c**) and step height (**d**) distributions of Pt(553). The values in red and the dashed red lines indicate the centre of each peak. For **a** and **c**, we obtained these values from Gaussian fits, with which we deconvoluted the peaks in the case of Pt(553). The statistical errors shown with grey error bars, which are calculated as the square root of each bin count, lead to uncertainties on the centre values (green arrows) as well as on the percentages of single, double and triple steps, which are reported in black on top of the corresponding peak.

interaction. The centre of the Gaussian distribution is at 21.9 ± 0.8 Å, which agrees with the theoretical terrace width of 22.4 Å. Moreover, Fig. 3b exhibits only one peak in the distribution, indicating that the steps on Pt(554) have monoatomic height.

In contrast, the terrace width distribution on Pt(553), shown in Fig. 3c, reveals not only one but three peaks, centred at 11.3 ± 0.5 Å, 20.6 ± 0.5 Å and 30 ± 1 Å. These peaks correspond to terraces with nominal, double and triple terrace widths, respectively, thus pointing to the presence of also double and triple steps. This again is supported by the step height distribution in Fig. 3d, which shows also three different peaks, centred at 2.25 Å (monoatomic step height), 4.50 Å (double step height) and 6.75 Å (triple step height).

From the percentages indicated on each peak in Fig. 3c,d, we extracted the corresponding averaged percentages of single (35 ± 4%), double (51 ± 5%) and triple (14 ± 3%) steps on Pt(553). We conclude that, while Pt(554) shows exclusively single steps and a terrace width around its nominal value, more than 65% of the steps on Pt(553) are bunched.

Origin of the step bunching instability

Whether a vicinal surface undergoes step bunching depends on the delicate balance between f_{step} and B_{step}, which may result in a lower total free energy f_{total} for the bunched configuration. Figure 4a shows f_{total} with and without the repulsive step–step interaction, calculated with equations (1) and (2) and plotted versus the terrace width. One can observe that the dependence of f_{total} on the terrace width is mainly given by f_{step}/L up to narrow terraces ($n = 8$), below which the step–step interaction starts to play an increasingly important role.

The surface configuration with double steps not only has terraces with twice of the nominal terrace width, but also has a different f_{step} and B_{step} compared with single steps, resulting in a different f_{total}. Figure 4b shows the energy ratio between a surface with double steps and a surface with single steps calculated at $T = 1{,}300$ K, which is around 100 K below the maximum temperature reached during our flame annealing (for the temperature dependence of this energy ratio, see Supplementary Notes 2 and 3 as well as Supplementary Fig. 6). As surface diffusion drops exponentially with temperature, we estimate that, upon further temperature decrease during the cooling down, the step configuration becomes frozen because of kinetic limitations. As an approximation, we also assumed for this calculation that the formation and kink energies of a double step ($f^0_{\text{double step}}$ and $f^0_{\text{double kink}}$, respectively) are exactly two times f^0_{step} and f^0_{kink} (ref. 22). In Supplementary Fig. 7, we show the dependence on the step bunching instability when varying these values, which we discuss in Supplementary Note 4. Moreover, we derived that the step–step interaction coefficient of double steps, $B_{\text{double step}}$, is 1.34 times larger than the one of single steps (see again Supplementary Note 2).

Figure 4b shows that, for our case, stepped surfaces with a terrace width larger than eight atomic rows are expected to be stable, while those with equal or narrower terraces can decrease the total free energy by the formation of step bunches. This is due to the lowering of the step–step repulsion when doubling the terrace width, as not only the step–step interaction term scales with L^{-3} (while the second term in equation (1) goes with L^{-1}) but also because $B_{\text{double step}} < 2B_{step}$

(refs. 10,23). Although this result is only indicative, as we used some assumptions and values from vacuum studies, it explains why Pt(554) has single steps while Pt(553) mainly has double steps. Moreover, we have EC-STM proof that Pt(533), with (100) steps and a nominal terrace width of 4 atom rows, also presents predominantly bunched steps. In addition, step bunching also explains the observation made in surface X-ray diffraction studies that flame-annealed Pt(311) and Pt(331) surfaces exhibit terraces wider than expected, although the authors refer to surface reconstruction rather than to step bunching[24,25].

Please note also that we cannot discard that the step bunching instability is induced by oxygen adsorption during surface preparation[1–4,6], which could lower $f_{\text{double step}}$, as we performed the flame annealing in air before transferring the sample for cooling down into a glass cylinder with an Ar + H_2 mixture. This would explain why Lang and Blakely observed with low-energy electron diffraction that even platinum stepped surfaces with a terrace width of only three atomic rows were stable if prepared in ultrahigh vacuum[1,2], while Hahn et al. showed that Pt(997) with a terrace width of nine atomic rows undergoes step bunching when annealing in the presence of oxygen[4].

Finally, we can discard that the surface morphology on Pt(553) changes notably with time while in the EC-STM, which reinforces our statement that the step bunches are formed during sample preparation with enhanced step mobility. Moreover, we observed the same step-bunched structure on Pt(553) at least at two applied potentials: 0.1 V, where H covers the surface, and 0.4 V in the double layer region, where nothing is specifically adsorbed on the surface (Supplementary Fig. 8). This indicates either that both the hydrogen adsorbed and the clean surface preserve the energetics of the most (thermodynamically) stable structure or that the surface is kinetically limited, and thus frozen, at room temperature and, thus, visible changes do not occur within the time span of our measurements. Our results differ from the ones reported in refs. 26,27 with a flame-annealed Ag(19 19 17) submerged in a $CuSO_4$ solution. These showed not only that the density of step bunches on this surface increases with time, but also that this increase occurs faster the higher the applied potential[28]. This indicates that the Ag(19 19 17) surface, as measured, did not reach thermodynamic equilibrium and that surface diffusion at room temperature is still high enough for step rearrangement. Alternatively, the chemisorption of sulfate or copper deposition as well as alloy formation could also have had an important role[29].

Effects of step bunching in electrocatalysis

Figure 5a shows the hydrogen desorption region from cyclic voltammograms of Pt(111) and Pt(111)-vicinal surfaces with (111) steps in 0.1 M $HClO_4$. All stepped surfaces present a broad feature below 0.4 V and a sharp peak at around 0.13 V, which relate to terrace and step sites, respectively[30]. Pt(553) and Pt(221) show, in addition, an extra peak at around 0.185 V that was previously attributed to hydrogen desorption from narrow terraces[31]. However, we know now that it is related to hydrogen desorption and its (partial) replacement with hydroxide at step bunches[32]. A similar peak is also observed on Pt(110)-vicinals with (111) steps[33], which supports further our insights. Pt(775) does not show this feature, but the potential shift of the single step peak (Supplementary Note 5 and Supplementary Fig. 9) suggests that also this surface exhibits (some) step bunching.

Step bunching also affects E_{pztc}. As E_{pztc} is closely related to the work function, one expects a linear decrease of E_{pztc} with the step density according to[11,27,34–36]

$$\Delta E_{\text{pztc}}\left(\frac{1}{L}\right) = E_{\text{pztc, stepped surface}} - E_{\text{pztc, (111)}} = -\frac{p_z}{\epsilon_0\, a\, L}, \qquad (4)$$

where ϵ_0 is the vacuum dielectric constant and p_z the dipole moment at the steps. However, the red curve in Fig. 5b (data extracted from refs. 7,32) shows that the initial linear dependency of E_{pztc} with step density starts to deviate for $n \leq 7$. This phenomenon was previously attributed to the decay of p_z due to the interference of the stress and electrical fields between closely spaced steps[37]. Evidently, as we know now that closely spaced steps bunch, resulting in wider terraces, the real explanation must be different. Mainly, step bunching results in a decrease of the ratio p_z/L, as L is doubled but $p_{z,\text{ double step}} << 2p_{z,\text{ single step}}$ (ref. 23). This leads to a higher E_{pztc} than expected.

Figure 5b shows in blue the local E_{pztc} at steps (data extracted from ref. 38), which is constant at low step densities but starts increasing at $n = 7$. As step bunches have a different p_z than single steps, this again suggests that the onset of step bunching starts with Pt(775).

Subsequently, we used both curves in Fig. 5b, our measured percentage of bunched steps on Pt(553), and equation (4) to calculate $p_{z,\text{ double step}}$. Knowing that $p_{z,\text{ single step}} = 0.14$ D (in 0.1 M $HClO_4$)[7] and

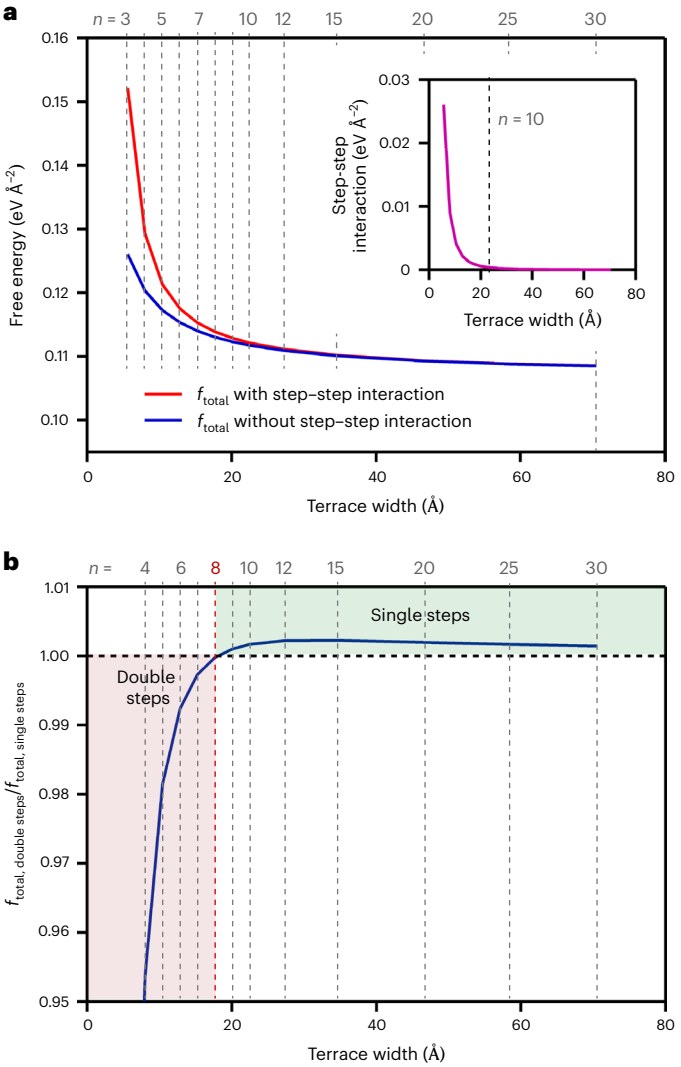

Fig. 4 | Thermodynamics of step bunching. a, f_{total} with step–step interaction (red), f_{total} without step–step interaction (blue) and step–step interaction (inset, in purple) as a function of the terrace width for $T = 1{,}300$ K. For the calculations, we used equations (1) and (2), with $f_{\text{terr}} = 1.07$ eV Å^{-2} from ref. 49 and the values of $f^0_{\text{step}} = 0.120$ eV Å^{-1} and $f^0_{\text{kink}} = 0.206$ eV from ref. 50. We extracted the step interaction parameter $B_{\text{step}} = 12.76$ eV Å^2 from the one reported in ref. 49, which we extrapolated to match with our temperature (Supplementary Note 2). **b**, The surface free energy ratio between configurations with double and single steps as a function of the terrace width. To calculate the surface free energy for the double steps, we reasonably approximated $f^0_{\text{double step}} = 2 \times f^0_{\text{step}} = 0.240$ eV Å^{-1} and $f^0_{\text{double kink}} = 2 \times f^0_{\text{kink}} = 0.412$ eV. We extracted $B_{\text{double step}} = 17.11$ eV Å^2 by scaling B_{step} with the ratio of the dipole moments of double steps and single steps, as explained in Supplementary Note 2.

https://doi.org/10.1038/s41929-024-01232-2

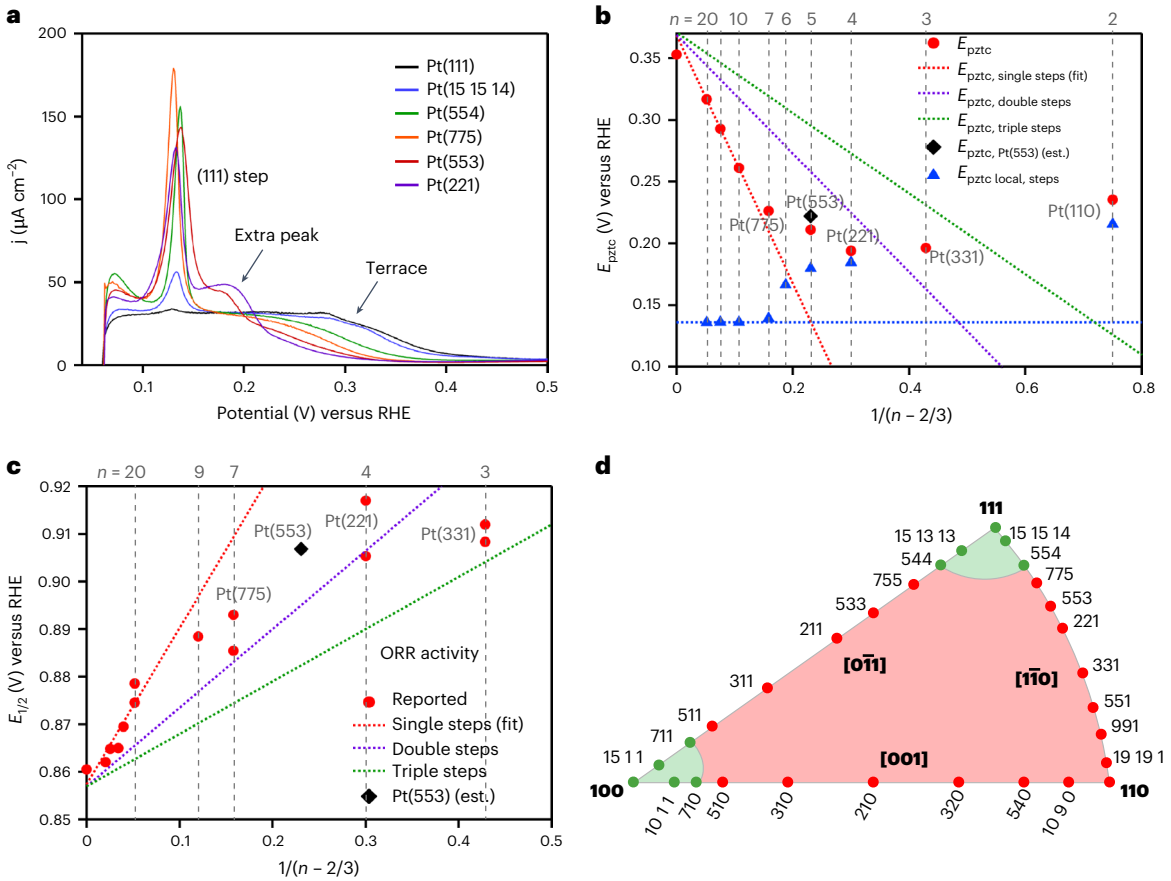

Fig. 5 | Effects of step bunching on platinum electrochemistry. a, The hydrogen desorption fingerprint of Pt(111) and (111)-vicinal surfaces with (111) steps recorded in 0.1 M $HClO_4$ at a scan rate of 50 mV s^{-1}. The peaks related to terraces, single (111) steps and step bunches, the latter only present on Pt(553) and Pt(221), are indicated. **b**, E_{pztc} (in red) and (local) E_{pztc} at step sites (in blue) versus the step density, extracted from refs. 7,32,38. The surfaces that undergo step bunching ($n \leq 7$) do not follow the linear decrease of E_{pztc} with step density shown in red. The dotted purple and green lines represent the expected trends of E_{pztc} assuming 100% double steps and 100% triple steps, respectively. The black diamond represents our estimation (est.) of E_{pztc} for Pt(553), calculated from a fit of the dipole moment for double steps. **c**, The ORR activity, represented by the half-wave potential, versus step density, extracted from refs. 8,9,40. The ORR activity clearly increases linearly with the step density for $n \geq 20$. **d**, A stereographic triangle showing the stable surfaces in green and the unstable ones in red. Pt(110) forms a (1 × 2) missing-row reconstruction[21,44], while Pt(100) is unreconstructed in electrolyte[45].

assuming that $p_{z,\,\text{triple step}} \approx p_{z,\,\text{double step}}$, we obtain $p_{z,\,\text{double step}} = 0.168$ D and $p_{z,\,\text{double step}} = 0.172$ D from the two curves, respectively. This means that the dipole moment of the double step is only ~21% larger than the one of the corresponding single step. To further confirm this, we use the average value of $p_{z,\,\text{double step}} = 0.170$ D together with the measured percentage of bunched steps and estimate E_{pztc} for Pt(553) (drawn with the black diamond), which is close to the value measured. The dotted purple and green lines represent the expected trends of E_{pztc} assuming 100% of double steps and 100% of triple steps, respectively. The fact that Pt(221) falls close to the purple line suggests that it has predominantly double steps, while Pt(331) has a mixture between double and triple steps. As explained above, surfaces with higher step density suffer from increased step–step interaction, which leads to a higher degree of step bunching for Pt(331).

On another topic, it is well known that the ORR in acidic media is most active at the concave sites situated at the lower step edge, where the OH_{ad} intermediate binds more weakly than on the (111) terraces[39,40]. Consequently, one would expect the ORR activity to increase (almost) linearly with the number of these concave sites and, thus, with step density (the effects of the Smouluchowski relaxation have a higher order dependency with the step separation and, thus, are less important[15–19]). However, Fig. 5c shows in red (data extracted from refs. 8,9,40) that the ORR half-wave potential ($E_{1/2}$), an activity descriptor, increases linearly with step density until $n < 9$.

As we have evidence that Pt(775), Pt(221) and Pt(331) undergo step bunching, this reduces the amount of lower step edge sites in approximation by a factor 1/2 if all steps would simply bunch into pairs (Fig. 2), and a factor 1/3 if all steps bunch into triplets. As these are the most active sites for the ORR, we expect an equivalent decrease of the activity. Therefore, we represent in Fig. 5c the expected ORR activity for Pt(553) (black diamond) as well as the expected trends assuming that all steps are bunched into either pairs (purple line) or triplets (green line). It is striking that Pt(221) falls close to the purple line, indicating once again that it presents mainly double steps. Meanwhile, the proximity of Pt(331) to the green line suggests a higher fraction of triple steps. According to this graph, Pt(775) has a rather large percentage of double steps, although this seems to be in contrast with the results from Fig. 5a,b, which suggest a small fraction. However, we also know that Pt(775) is at the edge of the step bunching instability (Fig. 5b) such that even slightly different sample preparation conditions (for example, annealing temperature, cooling gas composition and cooling speed) could lead to a large variation of the fraction of step bunches.

Finally, step bunching also impacts other structure-sensitive electrochemical reactions that are most active at step-related sites. Step bunches on Pt(111)-vicinals with $n \leq 5$ show a reduced activity towards both the hydrogen oxidation reaction[41] and the CO oxidation reaction[42]. By contrast, nitrate reduction shows a substantial increase for $n \leq 5$ (ref. 31), which suggests a more optimal binding of the reaction

intermediates at the bunched steps. Vacuum studies show that Pt(533), exhibiting (100) steps, undergoes step bunching during ammonia oxidation, resulting in a change in selectivity from producing N_2 to producing NO (ref. 43). Moreover, we have recent evidence that step bunching leads also to a decrease of the hydrogen adsorption as well as platinum oxidation at step sites. To provide a graphical representation of our insights, we built up a stereographic triangle in which we indicate the surfaces that are unstable towards step bunching (Fig. 5d and Supplementary Tables 1–3). This is derived on the basis of the information in the literature regarding the electrochemical behaviour of flame-annealed stepped platinum surfaces, together with this work and other characterization studies[21,24,25,44,45].

Conclusions

In this Article, we demonstrate that flame-annealed Pt(111)-vicinal electrodes with high step density undergo step bunching, which has a remarkable impact on the electrochemical behaviour of the surface. Our statistical analysis of the terrace width and the step height distribution shows that, while Pt(554) presents a regular array of single steps separated by the nominal distance, 51 ± 5% and 14 ± 3% of the steps on Pt(553), which has higher step density, are bunched into pairs and triplets, respectively. This instability originates from the highly repulsive step–step interaction between closely distanced steps, which is lowered by forming step bunches with larger spacing in combination with a dipole moment that is increased by only ~21% to 0.17 D for double steps, in comparison with the 0.14 D of single steps. The bunching must occur during surface preparation at high temperature, when the surface mobility is enhanced, as we did not observe notable changes of the surface structure during our EC-STM measurements, not even when switching the sample potential. Pt(111)-vicinal electrodes with bunched steps exhibit an extra peak at around 0.185 V in the hydrogen desorption fingerprint, as well as an unexpected, nonlinear trend of their E_{pztc} and ORR activity with their step density. Our insight challenges the common assumption in electrochemistry that all vicinal surfaces present a regular array of monoatomic-height steps and can successfully explain the anomalous step density-dependent trends reported in literature.

Methods

Electrochemistry

We recorded the cyclic voltammograms in a glass cell that we cleaned first with an acidic potassium permanganate solution and then with diluted piranha solution, before finally boiling it five times in ultrapure water (>18.2 MΩ cm, Millipore Milli-Q). For the measurements, we used a reversible hydrogen electrode (RHE) as the reference and a Pt wire (MaTeck) as the counter. Our working electrode was a high-quality (99.999% purity and polished <0.1°) platinum single crystal, either a Pt(111) (Surface Preparation Laboratory) or a (111)-vicinal surface with (111) steps (MaTeck). The latter can be described with the notation Pt(s)[n(111) × (111)], where n is the number of atomic rows on a single terrace. Before the measurements, we etched the platinum sample electrochemically (125 cycles at 50 Hz, ±2 V versus Pt) in an acidified 2.5 M $CaCl_2$ solution. Subsequently, we flame-annealed it (3 min at ~1,250 K) and immediately cooled it down in a 1:4 H_2/Ar mixture. We repeated this treatment three times, with the last annealing step at a slightly lower temperature (~50 K lower) to deplete the surface from contamination coming from the bulk. We performed all the cyclic voltammograms in an Ar-purged 0.1 M $HClO_4$ solution (Merck Suprapur), using a potentiostat from Bio-Logic (VSP-300).

Electrochemical scanning tunnelling microscopy

We recorded the STM images with a home-built EC-STM[46,47]. We used an RHE and a Pt coil as reference and counter electrodes, respectively, while the working electrode was either Pt(554) or Pt(553) with which we also recorded the cyclic voltammograms. We made the STM tips by electrochemical etching of a $Pt_{90}Ir_{10}$ wire (Goodfellow), and we coated them with electrophoretic paint (Clearclad HSR) and polyethylene to minimize the faradaic contributions in the tunnelling current. Before every measurement, we cleaned all the glassware and pipes following the procedure described in ref. 48 and we de-aerated the electrolyte (0.1 M $HClO_4$) with N_2 for at least 3 h.

Data availability

All the EC-STM images used for this study are available within the Article and its Supplementary Information. The EC-STM statistical data on the terrace widths and step heights are included as a source data file. The data files are also available from the corresponding author upon reasonable request. Source data are provided with this paper.

Code availability

The custom-made Python code for processing and analysing the EC-STM images is available from the corresponding author upon reasonable request.

References

1. Lang, B., Joyner, R. W. & Somorjai, G. A. Low energy electron diffraction studies of chemisorbed gases on stepped surfaces of platinum. *Surf. Sci.* **30**, 454–474 (1972).
2. Blakely, D. W. & Somorjai, G. A. The stability and structure of high miller index platinum crystal surfaces in vacuum and in the presence of adsorbed carbon and oxygen. *Surf. Sci.* **65**, 419–442 (1977).
3. Comsa, G., Mechtersheimer, G. & Poelsema, B. He-beam scattering study of the dynamics of oxygen induced reconstruction of the Pt(997) surface: I. Dynamics of double step formation and destruction. *Surf. Sci.* **119**, 159–171 (1982).
4. Hahn, E., Schief, H., Marsico, V., Fricke, A. & Kern, K. Orientational instability of vicinal Pt surfaces close to (111). *Phys. Rev. Lett.* **72**, 3378–3381 (1994).
5. Clavilier, J., Faure, R., Guinet, G. & Durand, R. Preparation of monocrystalline Pt microelectrodes and electrochemical study of the plane surfaces cut in the direction of the {111} and {110} planes. *J. Electroanal. Chem.* **107**, 205–209 (1980).
6. Herrero, E., Orts, J. M., Aldaz, A. & Feliu, J. M. Scanning tunneling microscopy and electrochemical study of the surface structure of Pt(10,10,9) and Pt(11,10,10) electrodes prepared under different cooling conditions. *Surf. Sci.* **440**, 259–270 (1999).
7. Climent, V., Gómez, R. & Feliu, J. M. Effect of increasing amount of steps on the potential of zero total charge of Pt(111) electrodes. *Electrochim. Acta* **45**, 629–637 (1999).
8. Kuzume, A., Herrero, E. & Feliu, J. M. Oxygen reduction on stepped platinum surfaces in acidic media. *J. Electroanal. Chem.* **599**, 333–343 (2007).
9. Gómez-Marín, A. M. & Feliu, J. M. Oxygen reduction on nanostructured platinum surfaces in acidic media: promoting effect of surface steps and ideal response of Pt(111). *Catal. Today* **244**, 172–176 (2015).
10. Williams, E. D. & Bartelt, N. C. Thermodynamics of surface morphology. *Science* **251**, 393–400 (1991).
11. Ibach, H. *Physics of Surfaces and Interfaces* (Springer, 2006).
12. Lapujoulade, J. The roughening of metal surfaces. *Surf. Sci. Rep.* **20**, 195–249 (1994).
13. Bartelt, N. C., Einstein, T. L. & Williams, E. D. The influence of step–step interactions on step wandering. *Surf. Sci. Lett.* **240**, L591–L598 (1990).
14. Gruber, E. E. & Mullins, W. W. On the theory of anisotropy of crystalline surface tension. *J. Phys. Chem. Solids* **28**, 875–887 (1967).
15. Smoluchowski, R. Anisotropy of the electronic work function of metals. *Phys. Rev.* **60**, 661–674 (1941).

16. Jayaprakash, C., Rottman, C. & Saam, W. F. Simple model for crystal shapes: step–step interactions and facet edges. *Phys. Rev. B* **30**, 6549–6554 (1984).
17. Lau, K. H. & Kohn, W. Elastic interaction of two atoms adsorbed on a solid surface. *Surf. Sci.* **65**, 607–618 (1977).
18. Marchenko, V. I. & Parshin, A. Y. Elastic properties of crystal surfaces. *Sov. Phys. JETP* **52**, 129–131 (1980).
19. Shilkrot, L. E. & Srolovitz, D. J. Elastic field of a surface step: atomistic simulations and anisotropic elastic theory. *Phys. Rev. B* **53**, 122–127 (1996).
20. Prévot, G., Steadman, P. & Ferrer, S. Determination of the elastic dipole at the atomic steps of Pt(977) from surface X-ray diffraction. *Phys. Rev. B* **67**, 245409 (2003).
21. Swamy, K., Bertel, E. & Vilfan, I. Step interaction and relaxation at steps: Pt(110). *Surf. Sci. Lett.* **425**, L369–L375 (1999).
22. Nelson, R. C., Einstein, T. L., Khare, S. V. & Rous, P. J. Energies of steps, kinks, and defects on Ag(100) and Ag(111) using the embedded atom method, and some consequences. *Surf. Sci.* **295**, 462–484 (1993).
23. Ishida, H. & Liebsch, A. Calculation of the electronic structure of stepped metal surfaces. *Phys. Rev. B* **46**, 7153–7156 (1992).
24. Nakahara, A., Nakamura, M., Sumitani, K., Sakata, O. & Hoshi, N. In situ surface X-ray scattering of stepped surface of platinum: Pt(311). *Langmuir* **23**, 10879–10882 (2007).
25. Hoshi, N. et al. Surface x-ray scattering of stepped surfaces of platinum in an electrochemical environment: Pt(331) = 3(111)–(111) and Pt(511) = 3(100)–(111). *Langmuir* **27**, 4236–4242 (2011).
26. Baier, S., Ibach, H. & Giesen, M. The instability of vicinal electrode surfaces against step bunching I: experiment. *Surf. Sci.* **573**, 17–23 (2004).
27. Ibach, H. & Schmickler, W. The instability of vicinal electrode surfaces against step bunching II: theory. *Surf. Sci.* **573**, 24–31 (2004).
28. Giesen, M. et al. The thermodynamics of electrochemical annealing. *Surf. Sci.* **595**, 127–137 (2005).
29. Magnussen, O. M. Ordered anion adlayers on metal electrode surfaces. *Chem. Rev.* **102**, 679–725 (2002).
30. Clavilier, J., El Achi, K. & Rodes, A. In situ characterization of the Pt(S)-[*n*(111)×(111)] electrode surfaces using electrosorbed hydrogen for probing terrace and step sites. *J. Electroanal. Chem.* **272**, 253–261 (1989).
31. Taguchi, S. & Feliu, J. M. Electrochemical reduction of nitrate on Pt(S)[*n*(111)×(111)] electrodes in perchloric acid solution. *Electrochim. Acta* **52**, 6023–6033 (2007).
32. Rizo, R. et al. Investigating the presence of adsorbed species on Pt steps at low potentials. *Nat. Commun.* **13**, 2550 (2022).
33. Souza-Garcia, J., Climent, V. & Feliu, J. M. Voltammetric characterization of stepped platinum single crystal surfaces vicinal to the (110) pole. *Electrochem. Commun.* **11**, 1515–1518 (2009).
34. Besocke, K., Krahl-Urban, B. & Wagner, H. Dipole moments associated with edge atoms; a comparative study on stepped Pt, Au and W surfaces. *Surf. Sci.* **68**, 39–46 (1977).
35. Trasatti, S. Work function, electronegativity, and electrochemical behaviour of metals: II. Potentials of zero charge and electrochemical work functions. *J. Electroanal. Chem. Interf. Electrochem.* **33**, 351–378 (1971).
36. Gómez, R., Climent, V., Feliu, J. M. & Weaver, M. J. Dependence of the potential of zero charge of stepped platinum (111) electrodes on the oriented step-edge density: electrochemical implications and comparison with work function behavior. *J. Phys. Chem. B* **104**, 597–605 (2000).
37. Ross, P. N. The role of defects in the specific adsorption of anions on Pt(111). *J. Chim. Phys.* **88**, 1353–1380 (1991).
38. Climent, V., Attard, G. A. & Feliu, J. M. Potential of zero charge of platinum stepped surfaces: a combined approach of CO charge displacement and N_2O reduction. *J. Electroanal. Chem.* **532**, 67–74 (2002).
39. Calle-Vallejo, F. et al. Finding optimal surface sites on heterogeneous catalysts by counting nearest neighbors. *Science* **350**, 185–189 (2015).
40. Calle-Vallejo, F. et al. Why conclusions from platinum model surfaces do not necessarily lead to enhanced nanoparticle catalysts for the oxygen reduction reaction. *Chem. Sci.* **8**, 2283–2289 (2017).
41. Kajiwara, R., Asaumi, Y., Nakamura, M. & Hoshi, N. Active sites for the hydrogen oxidation and the hydrogen evolution reactions on the high index planes of Pt. *J. Elecroanal. Chem.* **657**, 61–65 (2011).
42. Lebedeva, N. P., Koper, M. T. M., Feliu, J. M. & van Santen, R. A. Role of crystalline defects in electrocatalysis: mechanism and kinetics of CO adlayer oxidation on stepped platinum electrodes. *J. Phys. Chem. B* **106**, 12938–12947 (2002).
43. Scheibe, A., Günther, S. & Imbihl, R. Selectivity changes due to restructuring of the Pt(533) surface in the $NH_3 + O_2$ reaction. *Catal. Letters* **86**, 33–37 (2003).
44. Marković, N. M., Grgur, B. N., Lucas, C. A. & Ross, P. N. Surface electrochemistry of CO on Pt(110)-(1×2) and Pt(110)-(1×1) surfaces. *Surf. Sci.* **384**, L805–L814 (1997).
45. Kibler, L. A., Cuesta, A., Kleinert, M. & Kolb, D. M. In-situ STM characterisation of the surface morphology of platinum single crystal electrodes as a function of their preparation. *J. Electroanal. Chem.* **484**, 73–82 (2000).
46. Yanson, Y. I., Schenkel, F. & Rost, M. J. Design of a high-speed electrochemical scanning tunneling microscope. *Rev. Sci. Instrum.* **84**, 023702 (2013).
47. Rost, M. J. in *Encyclopedia of Interfacial Chemistry* 1st edn, Vol. 1 (ed. Wandelt, K.) 180 (Elsevier, 2018).
48. Jacobse, L., Huang, Y. F., Koper, M. T. M. & Rost, M. J. Correlation of surface site formation to nanoisland growth in the electrochemical roughening of Pt(111). *Nat. Mater.* **17**, 277–283 (2018).
49. Jeong, H. & Williams, E. D. Steps on surfaces: experiment and theory. *Surf. Sci. Rep.* **34**, 171–294 (1999).
50. Ikonomov, J., Starbova, K., Ibach, H. & Giesen, M. Measurement of step and kink energies and of the step-edge stiffness from island studies on Pt(111). *Phys. Rev. Lett.* **75**, 245411 (2007).

Acknowledgements

This work is part of the research programme TOP with project number 716.017.001, which is financed by The Dutch Organisation for Scientific Research (NWO).

Author contributions

M.T.M.K. and M.J.R. directed the project. M.T.M.K. acquired the funding. F.V.M. and M.J.R. conceived the idea and designed the experiments. F.V.M. performed the EC-STM measurements, the subsequent data analysis, and the theoretical calculations, which were supported by M.J.R. All authors participated in the discussion and interpretation of the results, as well as in writing and proofreading the article.

Competing interests

The authors declare no competing interests.

Additional information

Supplementary information The online version contains supplementary material available at https://doi.org/10.1038/s41929-024-01232-2.

Correspondence and requests for materials should be addressed to Marcel J. Rost.

Peer review information *Nature Catalysis* thanks Yunchang Liang and the other, anonymous, reviewer(s) for their contribution to the peer review of this work.